

RELATIONS BETWEEN RECONSTRUCTED 3D ENTITIES

Nicolas Pugeault

University of Edinburgh, United Kingdom
npugeaul@inf.ed.ac.uk

Sinan Kalkan, Florentin Wörgötter

University of Göttingen, Germany
sinan@chaos.gwdg.de, worgott@bccn-goettingen.de

Emre Baseski, Norbert Krüger

Syddansk University, Denmark
emre@mmmi.sdu.dk, norbert@mmmi.sdu.dk

Keywords: uncertainty, stereo, reconstruction, relations, geometry.

Abstract: In this paper, we first propose an analytic formulation for the position's and orientation's uncertainty of local 3D line descriptors reconstructed by stereo. We evaluate these predicted uncertainties with Monte Carlo simulations, and study their dependency on different parameters (position and orientation). In a second part, we use this definition to derive a new formulation for inter-features distance and coplanarity. These new formulations take into account the predicted uncertainty, allowing for better robustness. We demonstrate the positive effect of the modified definitions on some simple scenarios.

1 Introduction

Many computer vision applications make use of 3D objects models, provided to the system. Because these models are designed specifically for the task at hand, they can be precise, rich, and concise at the same time, and thereby simplify greatly reasoning problems. A common problem then is to relate the visually reconstructed 3D information about the scene with this accurate model knowledge. Local descriptors, as presented in section 3, have the advantage of being numerous and of describing the shape of the objects being witnessed. Their downside is that they describe only a small part of the object, and therefore are not very distinctive, and that objects are not uniquely described by local descriptors, due to sampling. Therefore it is advantageous to consider, beside the primitives themselves, relations between them: distance, collinearity, coplanarity, etc. For example, a square is described by parallel and orthogonal strings of collinear 3D-primitives, positioned at fixed distance one from the other — see (Baseski et al., 2007) for a discussion of visual representation with primitives' relations.

⁰A more detailed version of this study, containing all calculations, is available as a technical report, see reference (Pugeault et al., 2007).

When using exogenous knowledge about the objects in the scene, and the relations that define them, one need to consider the fact that primitives are only reconstructed up to a certain precision — see, e.g. (Hartley and Zisserman, 2000). Thus, inter-primitives relations can only be defined up to a certain tolerance that depends on primitive uncertainty. Moreover, the *selectivity* of a relation is inversely proportional to this tolerance. A primitive's uncertainty is function of image noise, calibration imprecision, and inaccuracies in primitive extraction, stereopsis, and reconstruction processes. This leads to large variations in primitives' uncertainties across the visual field. Assuming that a primitive's position and orientation error have Gaussian distributions, their uncertainties can be encoded by covariance matrices — see, e.g., (Clarke, 1998). A primitive's position uncertainty can be represented as an ovoid volume in space, centred on the correct position, and containing the plausible reconstructed positions; similarly, orientation's uncertainty forms a distorted cone. This is illustrated in Fig. 1. In this work we will model parameters uncertainty by their covariance matrices, and predict their propagation using an analytical first order approximation proposed by (Durrant-Whyte, 1988; Faugeras, 1993; Clarke, 1998). This is discussed in the first part of this paper, in section 4.

The computation of inter-primitives relations can

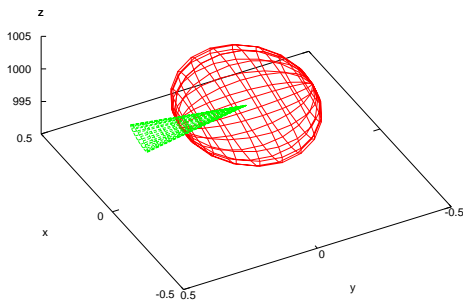


Figure 1: Illustration of the uncertainty. The red ovoid shows the position’s uncertainty, and the green cone the orientation’s uncertainty. The axes of the ellipse and the cone are computed from the Eigen-values and associated Eigen-vectors of the covariance matrices.

be severely affected by the imprecision in the 3D-primitives’ reconstruction. For example, consider the collinearity relation. If we make abstraction of the primitives’ imprecision, we can use the standard mathematical definition: two 3D-primitives are collinear if their orientation is parallel to the line that joins them. Now if we add some imprecision in the reconstruction process, these orientations will be slightly different. Normally this could be addressed by setting a threshold on the orientation difference, but the primitives’ uncertainty depends on parameters such as its orientation and position in space. In other words, there is no single threshold that can be set to define collinearity adequately for all cases. In the second part of this paper, in section 5, we will consider two relations: distance 5.1 and coplanarity 5.2. For each relation we propose a classic Euclidian formulation, and a second one taking into account the primitives’ uncertainty, in a manner reminiscent of the Mahalanobis distance. We compare the robustness (how regularly correct primitives pairs are identified) and selectiveness (how often primitives are erroneously paired) of the two formulations.

2 Literature review

The computation, and propagation of uncertainties has been studied for long, in particular in the field of photogrammetry, yet for the sake of concision, we will focus on studies related to computer vision. Verri and Torre (Verri and Torre, 1986) studied reconstructed points’ depth accuracy, and found that the length of the baseline is critical for the accuracy. Cri-

minisi and colleagues (Criminisi et al., 1997) studied point reconstruction uncertainty for planar surfaces. Rodríguez and Aggarwal (Rodríguez and Aggarwal, 1988) proposed to approximate reconstruction uncertainty by the *relative range error*, and Mandelbaum and colleagues (Mandelbaum et al., 1998) handle the depth uncertainty as a minimax risk confidence interval. Kamberova and Bajcsy (Kamberova and Bajcsy, 1998) make use of such intervals to reject data points. These works only consider the depth uncertainty in the case of point reconstruction. The proposed formulations do not allow for an easy inclusion of additional parameters. Hartley and Zisserman (Hartley and Zisserman, 2000) argue that the angle between the optical rays back-projected by a pair of image points yields a better estimate of the reconstructed point’s covariance than the disparity. Wolff (Wolff, 1989) discussed the stereo-reconstruction of lines, and propose an estimation of the reconstructed orientation’s uncertainty, demonstrating that reconstructing lines as an intersection of planes lead to a better accuracy than reconstructing the lines’ endpoints. The proposed analytical derivation is less general specific than the one used in this paper. Clarke (Clarke, 1998) also suggests to use Monte-Carlo simulation to estimate uncertainty, but points out the extreme computational cost of this approach. We argue that this approach is impractical when taking additional parameters into account (orientation, sparseness, cameras’ projection matrices), but provides an efficient way to evaluate an analytic derivation (see section 4.4). Heuel and colleagues (Heuel and Förstner, 2001) proposed a 3D line reconstruction using uncertain geometry. Their approach focuses on polyhedral objects, whereas the primitive-based framework used herein allows the representation of curved contours using local edge descriptors. This locality aspect requires us to reconstruct a position on the reconstructed 3D-line.

In this work, we first estimate the 2D-primitive’s extraction process uncertainty, then describe how it propagates to 3D-primitives, using the formulation proposed by (Durrant-Whyte, 1988; Faugeras, 1993; Clarke, 1998). Note that (Haralick, 2000) discussed the uncertainty propagation of processes based on function minimisation, applied to computer vision. Additional uncertainties stem from the projection matrices (these should be obtained from camera calibration), from stereo matching (an estimation is proposed here), and local curvature (that we will neglect in this paper). We model parameters’ uncertainties with their covariance matrices (see, e.g., (Clarke, 1998)). The most similar work is the study of Förstner and colleagues (Förstner et al., 2000) that use Grassman algebra to evaluate the confidence in several relations

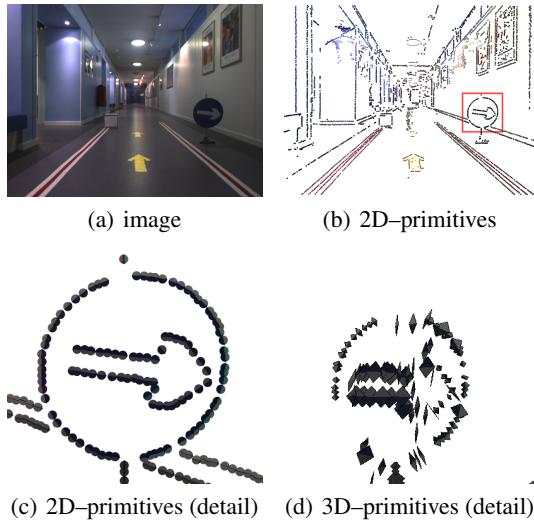


Figure 2: Illustration of the primitive-based vision framework presented in (Krüger et al., 2007) and used in this study.

between geometric entities. Their representation only handles global lines, though, and is inappropriate for local line descriptors. Moreover, they do not discuss the coplanarity nor distance relations.

3 The Primitive-Based Vision Framework

In this paper we make use of a framework proposed in (Krüger et al., 2007). This representation describes the image in terms of a sparse set of local, multi-modal line descriptors called *2D-primitives*. In this work we are only interested in the primitives' position (m) and local orientation (defined by the tangent vector t).¹ Therefore, primitives can be regarded as local tangents to image contours. In this work, primitives are extracted using the monogenic signal for the early vision processing, but it is worthwhile to note that Gaussian or Gabor wavelets could alternatively be used — see (Sabatini et al., 2006) for a discussion.

A stereo-pair of 2D-primitives allows to reconstruct a *3D-primitive*: a local 3D contour descriptor (which position is defined by M and orientation by the tangent vector T). Fig. 2 illustrates the 2D-primitive extraction and 3D-primitive reconstruction processes: (a) shows an image from an indoor navigation scenario; (b) shows the extracted 2D-primitives,

¹Primitives also hold some aspect parameters such as colour and phase, that are useful for, e.g., the stereo-matching process. See (Krüger et al., 2007).

with a detail on the traffic sign in (c); finally, (d) shows the 3D-primitives reconstructed by stereo.

4 Computing Uncertainties

Assuming that the error of a vector x has a Gaussian distribution, its uncertainty can be represented by its covariance matrix Λ_x . The uncertainties of the primitive extraction has been evaluated in (Krüger et al., 2007), and therefore we only need to study how this uncertainty is propagated by the stereo reconstruction process.

4.1 Uncertainty propagation

Given a function $y = f(m)$, where x and y are vectors with associated covariance matrices Λ_x and Λ_y , a first order Taylor series expansion gives us:

$$f(x + \Delta x) = f(x) + \nabla f(x) \cdot \Delta x + O(\|\Delta x\|^2) \quad (1)$$

from there (Clarke, 1998) derives that the relation between the covariance matrices of m and y is approximated by the relation

$$\Lambda_y \approx \nabla f \cdot \Lambda_x \cdot \nabla f^\top \quad (2)$$

where ∇f is the Jacobian matrix for the function f . This is the main result used hereafter to estimate uncertainties' propagation during stereo reconstruction. In the following we will equivalently denote $\Lambda = \sigma^2$ the variances of scalar values, and Λ the covariance matrices of vector quantities. Also, in the one-dimensional case, $\nabla f(x) = \frac{\partial f(x)}{\partial x}$ is the derivative of $f(x)$.

4.2 2D-Primitive Uncertainty

In (Krüger et al., 2007), the 2D-primitives' position and orientation error were evaluated. Although this error depends on local noise, texture and blur, we will assume in the following that these factors are constant. Because a 2D-primitive is a local line descriptor, the position error is only significant in the direction normal to this primitive's orientation.² Therefore, a primitive's position covariance is approximated by:

$$\Lambda_{\bar{m}} = \varepsilon^2 \cdot \begin{pmatrix} \sin(\theta) \\ \cos(\theta) \\ 0 \end{pmatrix} \cdot \Lambda_\theta \cdot \begin{pmatrix} \sin(\theta) & \cos(\theta) & 0 \end{pmatrix} \quad (3)$$

²Note that this is only true if the local curvature is small with regards to the position error. In general this assumption is true, as large curvatures lead to the extraction of corners, rather than lines primitives — see (Krüger et al., 2007).

where ε was evaluated in (Krüger et al., 2007) to $\varepsilon \simeq 0.0625$. Note that this covariance matrix describes the 2D-primitive’s homogeneous position \hat{m} , and therefore its third dimension’s variance is null. A 2D-primitive’s orientation variance is approximated to its mean square error, evaluated in (Krüger et al., 2007) to $\Lambda_\theta \simeq 9 \cdot 10^{-4}$ radians.

4.3 Reconstruction Uncertainty

We then study the propagation of 2D-primitives’ uncertainty during stereo-reconstruction, and estimate the resulting 3D-primitives’ uncertainty.

The relation between points in space and their projection in the image is defined by the camera’s projection matrix $\hat{P} = (P \ p)$ (see (Faugeras, 1993; Hartley and Zisserman, 2000)). In the following, and for the sake of simplicity, we assume that the cameras’ parameters are known, and their projection matrix exact $\Lambda_{\hat{P}} = 0_{12 \times 12}$. In the general case, the projection matrix will be estimated empirically through a process called *calibration* that provides its uncertainty as a by-product (Csurka et al., 1997). The precise derivation of the projection matrix uncertainty depends on the format of the uncertainty provided by the calibration software. In the case of the Matlab calibration toolbox (see (Bouguet, 2007)), the reader can find the derivation of the projection matrix uncertainty in the technical report (Pugeault et al., 2007).

Classical stereo-reconstruction tries to intersect two optical rays containing the possible origins of (or *back-projected* by) two corresponding points in two images. Because of imprecision, it is unlikely that the two lines intersect, and therefore the closest point to both rays is usually chosen. This approach is inadapted in the case of local line descriptors because the aperture problem makes reliable point matching impossible. On the other hand, (Wolff, 1989) discussed that accurate line matching could be achieved by intersecting the two planes back-projected from the lines in each image. Moreover, because primitives are *local* line descriptors we need a location along this line. This is obtained by intersecting the *line* containing the left 2D-primitive’s position possible origins with the *plane* containing the right 2D-primitive’s possible origins. The computation of the 3D-primitives’ uncertainty is using the uncertainty propagation formula in Eq. 2, as in (Clarke, 1998; Heuel and Förstner, 2001). The computation of the Jacobians will not be detailed here because of space constraints.

4.4 Evaluation

We evaluate the quality of the uncertainties predicted by the above formulae, using a Monte Carlo simulation in a simple scenario. The focal length is set to $f = 10^3$ and the baseline to $b = 100$, so that the optical centres of the cameras are located at $C_1 = (0, 0, 0)^\top$ and $C_2 = (b, 0, 0)^\top$.³

Consider a 3D-primitive at a location $\hat{M} = (0, 0, 100)^\top$ and with an orientation \hat{T} , projected on both image planes as $\hat{\pi}^l$ and $\hat{\pi}^r$. We apply a zero-mean Gaussian perturbation on position and orientation of those 2D-primitives, with a standard deviation of $\sigma = 0.25$ for position, and $\sigma = 0.03$ for orientation. This is according to the measured mean square error we assumed for our covariance prediction. Because we are only interested in the reconstruction uncertainty, we assume that $\hat{\pi}^l$ and $\hat{\pi}^r$ are accurate, and that all uncertainty comes from the added perturbation, and therefore the covariance of the projected 2D-primitive’s position is $\Lambda_m = 0.0625I_{2 \times 2}$; they have a vertical orientation (i.e., $\theta = 0$) with a variance of $\Lambda_\theta = 9 \cdot 10^{-4}$. Using a Monte Carlo simulation between predicted and measured covariance matrices $\xi = \frac{\|\Lambda' - \Lambda\|}{\|\Lambda'\|}$ of $\sim 3\%$ for position, and $\sim 4\%$ for orientation.

We then investigated how the 3D-primitive’s position and orientation impact the uncertainty thereof. We compared the trace $\text{tr}(\Lambda)$ of the reconstructed position’s covariance matrix (sum of the Eigenvalues), at different locations in space (Figs. 3(a), 3(b), and 3(c) for different values of the x (horizontal), y (vertical), and z (depth) coordinates) and for different pairs of 2D-orientations (Fig. 4(a)).

These figures show that the reconstructed position’s covariance is affected by the distance from the primitive to the cameras’ optical centres and by the right 2D-primitive’s orientation. The trace $\text{tr}(\Lambda_m)$ in Fig. 4(a) is mostly affected by θ_2 . This is due to the line reconstruction formula used in this work — see section 4.3. In this formulation, the right 2D-primitive’s orientation is used to resolve the ambiguity that stems from the aperture problem (we compute the intersection between a back-projected *left* ray and a back-projected *right* plane). This becomes impossible when the primitive’s orientation is the same that the epipolar line’s (in this case if $\theta_2 = \frac{\pi}{2}$), and therefore the reconstructed 3D-primitive’s position uncertainty increases to infinity for orientations close to $\frac{\pi}{2}$.

³These values were chosen for simplicity, but are nevertheless plausible: they are similar to the calibration parameters of an actual stereo camera system.

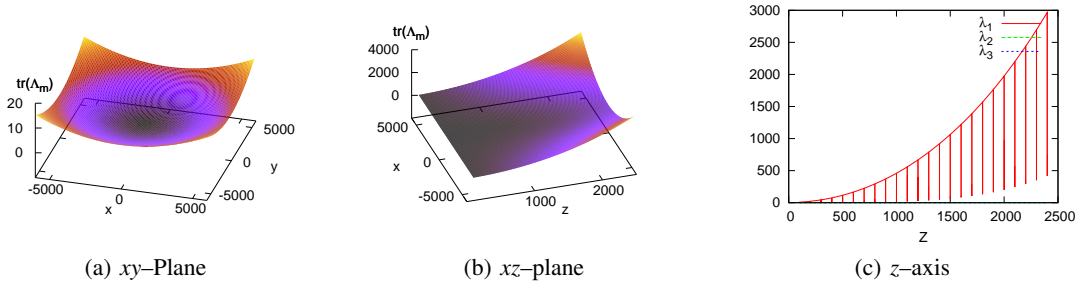


Figure 3: Traces of the covariance matrix Λ_M , for (a) different locations $M = (x, y, 100)^\top$ on the xy -plane; (b) different locations $M = (x, 0, z)^\top$ on the xz -plane; and (c) just considering the z -axis.

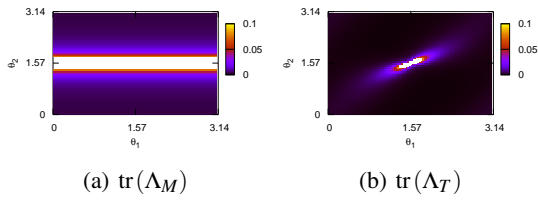


Figure 4: Effect of 2D-primitives' orientations on (a) the trace of Λ_M ; and (b) the trace of Λ_T .

We then evaluated the 2D-primitives' orientation impact on the reconstructed 3D-primitive's orientation uncertainty. Fig. 4 plots the trace of the reconstructed orientation's covariance matrix for a point located at $m = (0, 0, 100)^\top$, reconstructed from different 2D-primitives' orientations. In this figure we see that the reconstructed orientation uncertainty increases when either of the 2D-primitive's orientation becomes close to $\frac{\pi}{2}$. When both orientations become close to $\theta_1 = \theta_2 = \frac{\pi}{2}$ two primitives back-project the same plane $\mathcal{P}_1 = \mathcal{P}_2$, and therefore their intersection is undefined.

5 Design of 3D-Primitives Relations

In this section we consider distance and coplanarity between 3D-primitives, and propose definitions that take the uncertainties thereof into account, based on the Mahalanobis distance.

5.1 3D-Primitives normal distance

The first relation that we consider is the *normal distance* between two reconstructed 3D-primitives. The normal distance between two primitives Π_1 and Π_2 is defined as the distance from the line defined by primitive Π_1 position and orientation and primitive Π_2 po-

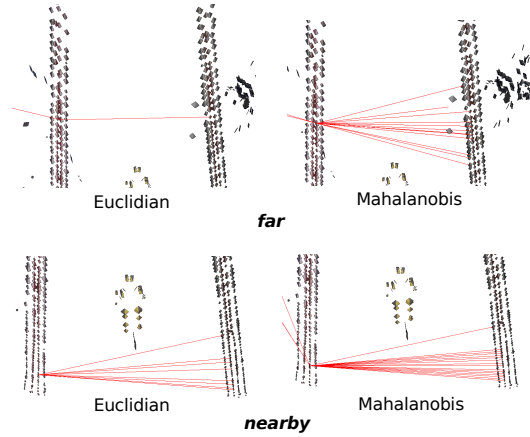
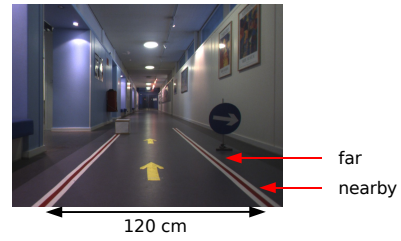


Figure 5: All primitives that satisfy a normal distance criterion with a selected primitive. The red lines indicate valid pairs.

sition. This is a useful measure when considering local line descriptors, as the exact positioning of a primitive along a line is effectively an artefact of sampling. Namely:

$$d_n = \|(M_2 - M_1) \times t_1\| \quad (4)$$

is the normal distance between Π_1 and Π_2 .

Consider the following scenario: We have three parallel vertical lines \mathcal{L}_A , \mathcal{L}_B , and \mathcal{L}_C . We have prior

world knowledge available, stating that there a distance of $a = 50$ between the lines \mathcal{L}_A and \mathcal{L}_B , and that \mathcal{L}_C is further away, at a distance of $a + b = 60$.

Consider three primitives, located at points $M_A = (100, 100, z)^\top \in \mathcal{L}_A$, $M_B = M_A + \mathbf{u} \in \mathcal{L}_B$ ($\mathbf{u} = (a, 0, 0)^\top$) and $M_C = (a + b + 100, 100, z)^\top \in \mathcal{L}_C$, all vertically oriented. These points' projections on both image planes are subjected to a zero-mean Gaussian perturbation applied to the projected 2D-primitives' position and orientation, with a standard deviation of $\sigma = 0.25$ and $\sigma = 0.03$ respectively. Then we reconstruct the 3D-primitives Π_i as described in section 4.3. We want to use our world knowledge to identify the primitives Π that belong to \mathcal{L}_A , \mathcal{L}_B , and \mathcal{L}_C . This is illustrated in a concrete scenario in Fig. 5. In this scenario, we know that the two red lines on the ground, delimiting the road, are parallel and separated by a distance a of 120cm. Using this world knowledge, we search for pairs of primitives that are separated by this distance, plus or minus 10cm. The figure shows the valid pairs for nearby and far 3D-primitives. In each case the red lines indicate with which other primitive it forms a valid pair according to each definition for distance.

We compare the performance of different distance measures for this task:

Euclidian Distance Threshold (E): We defined the threshold on the Euclidian distance as follows:

$$|d_n(\Pi_1, \Pi_2) - a| < \alpha^2 \quad (5)$$

where $d_n(\Pi_1, \Pi_2)$ stands for the normal distance between Π_1 and Π_2 , as defined in Eq. (4).

Mahalanobis Distance (M): The second criterion is based on the Mahalanobis distance:

$$(d_n(\Pi_1, \Pi_2) - a)^2 \cdot \Lambda_{dn} < \beta \quad (6)$$

where Λ_{dn} is the variance of the computed normal distance that comes directly from the uncertainty of Π_1 and Π_2 — see technical report (Pugeault et al., 2007) for a full derivation.

5.1.1 Evaluation

We compared the performance and robustness of both formulations using artificial images. We set $a = 50$, $b = 5$, $\alpha = 20$, and $\beta = 5$. The results are summarised in Fig. 6, the true positives curves (ETP and MTP) express the ratios of experiments wherein the reconstructed 3D-primitives A' and B' comply with the criterion (respectively E and M). The false positive curves (EFP and MFP) express the ratios of experiments wherein the reconstructed 3D-primitives A'

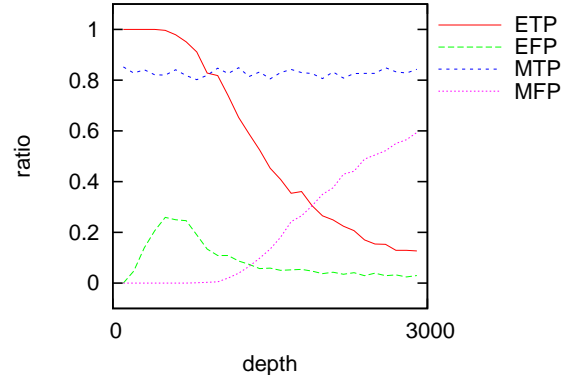


Figure 6: Comparison of the robustness of Euclidian (E) and Mahalanobis (M) distances, for the values $a = 50$, $b = 5$, $\alpha = 20$, and $\beta = 5$.

and C' satisfy the criterion. In this figure, we see that the number of true positive of the Euclidian criterion (ETP) decreases with depth.⁴ On the other hand, the ratio of true positive (MTP) is stable for the Mahalanobis distance. The false positives (MFP) increase progressively for large uncertainties, when the distribution of B and C overlap significantly. This shows that the normalised Mahalanobis distance is better suited for drawing spatial relations between reconstructed 3D-primitives.

This trend is illustrated qualitatively on real images in Fig. 5. There we have the values: $a = 120$, $\alpha = 10$, and $\beta = 0.5$.

5.2 Coplanarity relation

The second relation we studied is the coplanarity between two reconstructed 3D-primitives. As before, we consider three 3D-primitives, A , B , and C , with $\text{cop}(A, B) = 1$ and $\text{cop}(A, C) \simeq 0.70$ — this means an angle of $\frac{\pi}{4}$. The 3D-primitives are projected onto the image planes as before, the same Gaussian perturbation is applied, and both coplanarity criteria are applied to the reconstructed 3D-primitives Π_i .

Coplanarity is defined as follows:

$$\text{cop}(\Pi_1, \Pi_2) = (V \times T_1) \cdot (V \times T_2) \quad (7)$$

where $V = \frac{1}{\|M_2 - M_1\|} \cdot (M_2 - M_1)$. By using Eq.(2) in Eq.(7) we obtain the variance of the coplanarity mea-

⁴Note that the performance of the Euclidian distance (E) could be improved for a certain region of the space by altering α . Nonetheless, the general trend will be the same: larger α lead to more false positives for nearby structures, and the number of true positives tend to zero for far structures.

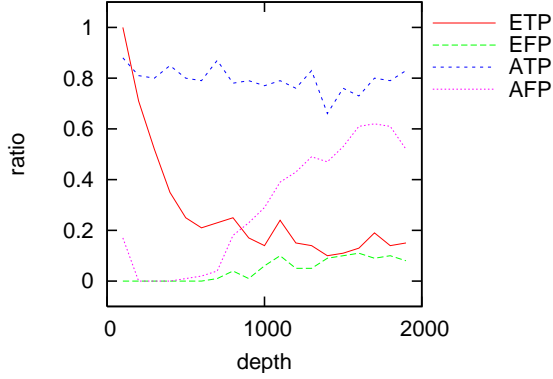


Figure 7: Proportion of coplanar pairs correctly labelled, using a fixed (E) and a variance dependent threshold (A), respectively.

sure:

$$\Lambda_{\text{cop}} = \begin{pmatrix} \eta_2^\top & \eta_1^\top \end{pmatrix} \cdot \begin{pmatrix} \Lambda_{V \times T_1} & \\ & \Lambda_{V \times T_2} \end{pmatrix} \cdot \begin{pmatrix} \eta_2 \\ \eta_1 \end{pmatrix} \quad (8)$$

with $\eta_i = V \times T_i$ the normal to the plane formed by the orientation T_i and the points M_1 and M_2 . Therefore, we propose the two following criteria for coplanarity:

Euclidian Coplanarity: The first definition simply applies a threshold on the coplanarity value:

$$1 - \text{cop}(\Pi_1, \Pi_2) < \alpha \quad (9)$$

Mahalanobis coplanarity: The second definition makes use of the estimated coplanarity variance to derive a Mahalanobis-like criterion:

$$\Lambda_{\text{cop}} \cdot (1 - \text{cop}(\Pi_1, \Pi_2))^2 < \beta \quad (10)$$

These two criteria, in Eq. 9 and 10, are compared in Fig 7, for values $\alpha = 0.01$ and $\beta = 0.5$. In this figure: ETP is the ratio of cases where Eq. 9 is verified between A' and B' , EFP where it is between A' and C' ; ATP the ratio where Eq. (10) is satisfied between A' and B' and AFP the ratio where it is satisfied between A' and C' . In Fig. 7 we see that the ratio ETP reduces quickly with the increase of depth. The ATP ration, on the other hand, is stable, while the AFP ratio increases with depth. This shows that the variance adapted threshold is a more robust criterion for reconstructed features' coplanarity than the naive Euclidian criterion, and this across a wide range of depth.

The result is further illustrated in Fig. 8. We see that when using the Mahalanobis version, the coplanar structures (red) are more densely connected than when using the Euclidian threshold, thus coplanarity

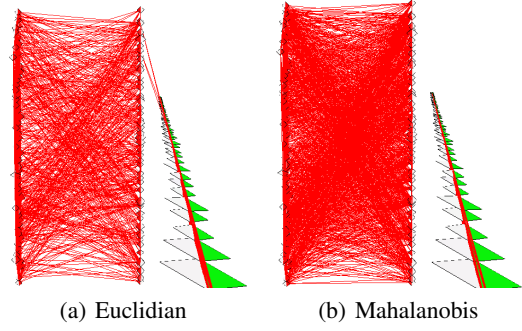


Figure 8: Illustration of the coplanar pairs extracted. The red lines show the primitives coplanar near (bottom) and far (top) from the camera.

is more reliably asserted. Furthermore, it is visible that the Euclidian criterion interpretes some of the farther green primitives as coplanar with the red ones.

6 Conclusion

This paper presented an analytical derivation of the uncertainty propagation in a vision framework using the primitives proposed by (Krüger et al., 2007), and the scene description in terms of inter-primitives relations discussed in (Baseski et al., 2007).

In a first part we discussed how image and calibration uncertainty propagates during the reconstruction process. This result, although classic in nature (e.g., (Clarke, 1998)), allowed us to formalise the peculiarities in the uncertainty space that stems from our use of local line descriptors (mainly its strong dependence on 2D orientation). The derivation presented here is specific to the representation proposed in (Krüger et al., 2007), yet it could easily be adapted to other line-based features. The advantage of an explicit analytic formulation of the uncertainty is, it allows us to accurately model the whole complexity of the uncertainty space. Estimating such a high dimensional space by Monte Carlo simulation would be impractical. This analytic derivation of uncertainty propagation was demonstrated to be accurate by Monte Carlo simulations.

The second and most important part of this paper considers inter-primitives geometric relations, focusing on the cases of normal distance and coplanarity. In (Baseski et al., 2007) it was discussed that such relations form a good base for interpreting visual information. Moreover, such relations form a way to provide prior geometrical knowledge about the scene, and compare this prior knowledge with the reconstructed 3D representation. Such relations need to

allow for a certain imprecision in the 3D-primitives, imprecision that is itself a function of the parameters thereof. The 3D-primitives' uncertainties computed in the first part were used to design alternative formulations of those relations that take uncertainty into account. The new formulations were shown to detect geometric relations in a more robust fashion than the naive Euclidian ones, and across wide ranges of depth.

We direct the reader interested in the detailed derivation of the uncertainties discussed in this paper towards the more detailed technical report (Pugeault et al., 2007). Future work includes defining a complete set of relations, and using it to formulate world knowledge in concrete scenarios.

Acknowledgements: This work was funded by the European project (DRIVSCO, 2009).

REFERENCES

- Baseski, E., Pugeault, N., Kalkan, S., Kraft, D., Wörgötter, F., and Krüger, N. (2007). A scene representation based on multi-modal 2D and 3D features. In *3D Representation for Recognition Workshop (in conjunction with ICCV)*.
- Bouguet, J.-Y. (2007). Camera Calibration Toolbox for Matlab. http://www.vision.caltech.edu/bouguetj/calib_doc/.
- Clarke, J. C. (1998). Modelling uncertainty: A primer. Technical report, Department of Engineering Science, Oxford University.
- Criminisi, A., Reid, I., and Zisserman, A. (1997). A plane measuring device. In *Proceedings of the British Machine Vision Conference*.
- Csurka, G., Zeller, C., Zhang, Z., and Faugeras, O. (1997). Characterizing the Uncertainty of the Fundamental Matrix. *Computer Vision and Image Understanding*, 68(1):18–36.
- DRIVSCO (2006-2009). *DRIVSCO: Learning to Emulate Perception-Action Cycles in a Driving School Scenario (FP6-IST-FET, contract 016276-2)*.
- Durrant-Whyte, H. F. (1988). Uncertain Geometry in Robotics. *IEEE Journal of Robotics and Automation*, 4(1):23–31.
- Faugeras, O. (1993). *Three-Dimensional Computer Vision*. MIT Press.
- Förstner, W., Brunn, A., and Heuel, S. (2000). Statistically testing uncertain geometric relations. In Sommer, G., Krüger, N., and Perwass, C., editors, *Mustererkennung 2000*, pages 17–26. DAGM, Springer.
- Haralick, R. M. (2000). Propagating covariance in computer vision. In *Proceedings of the Theoretical Foundations of Computer Vision, TFCV on Performance Characterization in Computer Vision*, pages 95–114, Deventer, The Netherlands, The Netherlands. Kluwer, B.V.
- Hartley, R. and Zisserman, A. (2000). *Multiple View Geometry in Computer Vision*. Cambridge University Press.
- Heuel, S. and Förstner, W. (2001). Matching, reconstructing and grouping 3d lines from multiple views using uncertain projective geometry. In *CVPR '01*. IEEE.
- Kamberova, G. and Bajcsy, R. (1998). Sensor Errors and the Uncertainties in Stereo Reconstruction. In K. Bowyer and P. Jonathon Phillips, editor, *Empirical Evaluation Techniques in Computer Vision*. IEEE Computer Soc. Press.
- Krüger, N., Pugeault, N., and Wörgötter, F. (2007). Multi-modal primitives: local, condensed, and semantically rich visual descriptors and the formalization of contextual information. Technical Report 2007-4, Robotics Group Maersk Institute, University of Southern Denmark.
- Mandelbaum, R., Kamberova, G., and Mintz, M. (1998). Stereo depth estimation: a confidence interval approach.
- Pugeault, N., Kalkan, S., Baseski, E., Wörgötter, F., and Krüger, N. (2007). Reconstruction uncertainty and 3d relations. Technical Report 6, Maersk Mc-Kinney Moller Institute, University of Southern Denmark.
- Rodríguez, J. J. and Aggarwal, J. K. (1988). Quantization error in stereo imaging. In *Proceedings of the CVPR*.
- Sabatini, S., Gastaldi, G., Solari, F., Pauwels, K., van Hulle, M., Díaz, J., Ros, E., Pugeault, N., and Krüger, N. (2006). Compact and accurate early vision processing in the harmonic space. In *2nd International Conference on Computer Vision Theory and Applications*.
- Verri, A. and Torre, V. (1986). Absolute depth estimate in stereopsis. *Journal of Optical Society of America*, 3:297–299.
- Wolff, L. B. (1989). Accurate measurements of orientation from stereo using line correspondence. In *IEEE Computer Society Conference on Computer Vision and Pattern Recognition (CVPR)*.